

---

---

# Therapeutic Efficacy and Tumor Dose Estimations in Radioimmunotherapy of Intraperitoneally Growing OVCAR-3 Cells in Nude Mice with $^{211}\text{At}$ -Labeled Monoclonal Antibody MX35

Jörgen Elgqvist, MSc<sup>1</sup>; Håkan Andersson, MD, PhD<sup>2</sup>; Tom Bäck<sup>1</sup>; Ragnar Hultborn, MD, PhD<sup>2</sup>; Holger Jensen, PhD<sup>3</sup>; Börje Karlsson, PhD<sup>1</sup>; Sture Lindegren, PhD<sup>1</sup>; Stig Palm, PhD<sup>1</sup>; Elisabet Warnhammar<sup>2</sup>; and Lars Jacobsson, PhD<sup>1</sup>

<sup>1</sup>Department of Radiation Physics, The Sahlgrenska Academy at Göteborg University, Göteborg, Sweden;

<sup>2</sup>Department of Oncology, The Sahlgrenska Academy at Göteborg University, Göteborg, Sweden;

and <sup>3</sup>PET and Cyclotron Unit, Rigshospitalet, Copenhagen, Denmark

---

The purpose of this study was to investigate the therapeutic efficacy of—and to estimate the absorbed dose to—tumor cells from radioimmunotherapy (RIT) in an ovarian cancer model using the  $\alpha$ -particle-emitting nuclide  $^{211}\text{At}$  labeled to monoclonal antibody (mAb) MX35. Previous studies on mAb MOv18 did not allow for dosimetry because of antigen shedding in vitro. **Methods:** Five-week-old female nude BALB/c *nu/nu* mice were inoculated intraperitoneally with  $1 \times 10^7$  cells of the human tumor cell line OVCAR-3. Three weeks later, the animals were given approximately 400, 800, or 1,200 kBq of  $^{211}\text{At}$ -labeled mAb MX35 intraperitoneally. As controls, one group of animals was injected with unlabeled mAb and another group was injected with phosphate-buffered saline (PBS). Another group was given approximately 400 kBq of  $^{211}\text{At}$  labeled to the previously investigated mAb MOv18 for efficacy comparison. Two months after treatment, the animals were sacrificed and the presence of macroscopic and microscopic tumors, as well as ascites, was determined. The absorbed dose to tumor cells on the peritoneal surface was estimated in terms of the sum of a specific and a nonspecific contribution. The specific contribution, arising from mAbs binding to the antigenic sites on the cell membrane, was calculated using a dynamic compartment model developed in-house and Monte Carlo software. The model used as input values the number of mAbs injected into the abdominal cavity,  $N_{\text{mAb}}$ , the specific activity,  $A_{\text{sp}}$ , the association rate constant,  $k_{\text{on}}$ , and the maximal number of mAbs bound per cell,  $B_{\text{max}}$ —all determined by in vitro experiments. This specific component of the absorbed dose was calculated for assumed cell cluster sizes with radii of 25, 50, and 100  $\mu\text{m}$ . The nonspecific contribution to the absorbed dose was derived from unbound mAbs freely circulating in the abdominal cavity, also using the Monte Carlo software. **Results:** In the control

groups given unlabeled MX35 or PBS, all 18 animals had ascites, 6 of 9 animals in each group had macroscopic tumors, and all animals had microscopic growth. In the 3 groups given different amounts of  $^{211}\text{At}$ -MX35, only 3 of 25 animals developed ascites. None of these animals had any sign of macroscopic tumors, but 8 had microscopic growth. In the group given  $^{211}\text{At}$ -MOv18, no animals had ascites or macroscopic tumors, but 3 of 10 animals had microscopic tumors. After injecting 400 kBq of  $^{211}\text{At}$ -MX35, the absorbed dose due to specific binding, for a cell cluster with a radius of 50  $\mu\text{m}$ , ranged from 413 to 223 Gy between 0- and 45- $\mu\text{m}$  distance from the cluster center, assuming a homogeneous distribution of  $^{211}\text{At}$ -MX35 in the cluster. The contribution from unbound  $^{211}\text{At}$ -MX35 and  $^{211}\text{At}$ -MX35 only distributed on the cluster surface, for this cluster size, ranged from 7 to 14 Gy and from 29 to 94 Gy, between 0- and 45- $\mu\text{m}$  distance from the cluster center, respectively. The calculated total absorbed doses are in a clinically relevant range and were effective as verified in the nude mice with subclinical intraperitoneal growth of OVCAR-3 cells. **Conclusion:**  $^{211}\text{At}$ -MX35 injected intraperitoneally exhibits a high efficacy when treating micrometastatic growth of the ovarian cancer cell line OVCAR-3 on the peritoneum of nude mice.

**Key Words:** radioimmunotherapy; MX35;  $^{211}\text{At}$ ; astatine;  $\alpha$ -particle

**J Nucl Med 2005; 46:1907–1915**

---

**R**adioimmunotherapy (RIT) is attracting increasing interest as new monoclonal antibodies (mAbs) are being introduced for clinical use. Ovarian cancer is usually limited to the peritoneal cavity, which allows a regional, intraperitoneal approach, lessening side effects.

Several studies have been performed on the therapeutic efficacy of  $\beta$ -emitters—primarily  $^{90}\text{Y}$ - and  $^{131}\text{I}$ -labeled to mAbs—in animals and humans with rather poor results (1–8). In nude mice with intraperitoneal growth of ovarian

---

Received Jan. 25, 2005; revision accepted Aug. 1, 2005.

For correspondence or reprints contact: Jörgen Elgqvist, MSc, Department of Radiation Physics, The Sahlgrenska Academy at Göteborg University, SE-413 45 Göteborg, Sweden.

E-mail: jorgen.elgqvist@radfys.gu.se

cancer, a delay in tumor progression or prolonged survival has been observed after intraperitoneal injection of anti-CA 125 mAb labeled to  $^{90}\text{Y}$ -labeled biotinylated liposomes (1), murine mAb HMFG1 labeled with  $^{90}\text{Y}$ ,  $^{186}\text{Re}$ , or  $^{131}\text{I}$  (2), and  $^{90}\text{Y}$ -labeled human IgM (3). However, there were no signs of complete remission of long-term duration in these studies. In clinical studies (4–8), the therapeutic response has been moderate; however, indications of some benefit to patients with minimal disease at the time of RIT have been reported (7).

Because of the fact that the  $\beta$ -emitting radionuclides mentioned have a range that is too long for the treatment of microscopic tumors, we believe it is of great interest to thoroughly investigate the therapeutic efficacy using  $\alpha$ -particle emitters labeled to mAbs when treating microscopic disease on the peritoneum. In this study we used the  $\alpha$ -particle emitter  $^{211}\text{At}$ , with a half-life of 7.2 h, a mean range in tissue of 62  $\mu\text{m}$ , and a mean linear energy transfer (LET) of 111 keV/ $\mu\text{m}$ . The short half-life of this radionuclide makes it ideal for local treatment, as the target cells are easily reached and the transfer of the radiotracer to the systemic circulation is delayed. Also, the short range ensures a significant absorbed dose to very small cell clusters or even single cells (9). The high LET of the  $\alpha$ -particles implies a higher relative biological effectiveness (RBE) than low-LET radiation. Therefore,  $^{211}\text{At}$  seems to be an appropriate radionuclide, when labeled to tumor-specific mAbs, for the treatment of micrometastatic growth on the peritoneum. We have previously demonstrated the high efficacy of  $^{211}\text{At}$ -labeled MOv18 on the ovarian cancer cell line OVCAR-3 in vitro and in vivo in a micrometastatic model (10–13).

In the present study we used mAb MX35, which binds to a 95-kDa glycoprotein, expressed strongly and homogeneously on 90% of human epithelial ovarian cancers (14). The object of the study was to establish a basis for clinical studies with this antibody, labeled to  $^{211}\text{At}$ . Thus, the main aim was to determine the therapeutic efficacy of  $^{211}\text{At}$ -MX35 in our established micrometastatic model, in comparison with the previously studied MOv18. The second aim was to estimate the absorbed dose to the micrometastases, to understand the therapeutic outcome. Absorbed dose calculations are generally based on repeated measurements of the radionuclide content in the tissue of interest; however, when such measurements are technically difficult or impossible, biokinetic models may be used. This is obviously the case for single cells and small cell clusters in the peritoneal cavity.

The parameters used in our biokinetic model, a dynamic compartment model, were determined by in vitro measurements of the association rate constant,  $k_{\text{on}}$ , and the maximal number of mAbs bound per cell,  $B_{\text{max}}$ , for MX35 and the OVCAR-3 cells. These 2 parameters, together with knowledge of the specific activity,  $A_{\text{sp}}$ —that is, the fraction of mAbs carrying  $^{211}\text{At}$  atoms—were then used in the dynamic compartment model in which the cumulated activity,  $\tilde{A}$  [ $\text{Bq} \times \text{s}$ ], at the surface of the tumor cells was calculated.

To be able to estimate the absorbed dose, software described previously (15) was modified for dosimetry on and within cell clusters. The software uses stopping-power values of  $\alpha$ -particles in liquid water (16) for Monte Carlo–derived microdosimetry. The absorbed dose resulting from  $^{211}\text{At}$ -labeled mAbs not bound to the tumor cells, but circulating free in the abdominal fluid and phosphate-buffered saline (PBS) surrounding the cells, was also calculated.

## MATERIALS AND METHODS

### Radionuclide

$^{211}\text{At}$  was produced by the  $^{209}\text{Bi}(\alpha, n)^{211}\text{At}$  reaction in a cyclotron (Scanditronix MC32 at the PET and Cyclotron Unit, Rigshospitalet, Copenhagen, Denmark) by irradiating a  $^{209}\text{Bi}$  target with 28-MeV  $\alpha$ -particles for 4 h with a beam current of approximately 18  $\mu\text{A}$ , resulting in an  $^{211}\text{At}$  activity of 900–1,100 MBq at the end of the irradiation. The target was prepared on  $30 \times 28 \times 5$  mm aluminum backings at the Department of Physics, Chalmers University of Technology, Göteborg, Sweden, and had a  $^{209}\text{Bi}$  layer thickness of 19–24  $\mu\text{m}$ . To stabilize this  $^{209}\text{Bi}$  layer and to prevent diffusion of the  $^{211}\text{At}$  produced during irradiation, an additional layer of 4- to 7- $\mu\text{m}$  aluminum was added on top of the  $^{209}\text{Bi}$  layer. After irradiation, the target was transported to the Department of Radiation Physics, The Sahlgrenska Academy at Göteborg University, Sweden, by car within 4 h for the final refinement of  $^{211}\text{At}$ . Upon arrival in Göteborg, the  $^{211}\text{At}$  was isolated using a dry-distillation procedure previously described by Lindegren et al. (17).

### mAbs

Two mAbs were used: MX35 and MOv18. MX35 is a murine IgG1 class mAb of about 150 kDa, developed and characterized at the Sloan-Kettering Institute (New York, NY), directed toward a cell-surface glycoprotein of about 95 kDa expressed by OVCAR-3 cells (18). The antigen is expressed strongly and homogeneously on 90% of human epithelial ovarian cancers (14). The mAb was provided by Dr. Kenneth Lloyd (Memorial Sloan-Kettering Cancer Center, New York, NY). MOv18 is also a murine IgG1 class mAb of about 150 kDa first characterized by Miotti et al. (19). It recognizes a membrane folate-binding glycoprotein of about 38 kDa and reacts with about 90% of human ovarian carcinomas (20). The antibody was provided by Professor S.O. Warnar (Centocor B/V, Leyden, The Netherlands).

### Antibody Labeling

mAbs were labeled with  $^{211}\text{At}$  using the intermediate labeling reagent *N*-succinimidyl-3-(trimethylstannyl)benzoate (*m*-MeATE) essentially as previously described (21). Briefly, the  $^{211}\text{At}$ , in 10 mmol/L NaOH, isolated from the irradiated target was added to a mixture of *m*-MeATE and *N*-iodosuccinimide in methanol:1% acetic acid. This solution was then incubated for 10 min at room temperature and the labeling reaction was stopped by adding sodium ascorbate. The mAb, MX35 or MOv18, was then added to the labeling mixture and conjugation was allowed to proceed for 20 min at room temperature. Finally, the mAb fraction was isolated using a NAP-5 column (Amersham Biosciences), resulting in a specific activity of  $134 \pm 25$  kBq/ $\mu\text{g}$  mAb. The radiochemical yields were in the range of 25%–40%, and the radiochemical purity was always >95% as determined by methanol precipitation and gel-permeability chromatography.

## Cell Line

The cell line OVCAR-3 (NIH:OVCAR-3: National Institutes of Health ovarian cancer cell line 3) was derived from the ascites of a patient with a poorly differentiated serous ovarian cancer by Hamilton et al. (22). In nude mice, it grows both subcutaneously and intraperitoneally, the latter closely mimicking the human disease, with peritoneal carcinomatosis and ascites. The cell line was obtained from the American Type Culture Collection. The cells were cultured in T-75 culture flasks at 37°C in a humidified atmosphere with RPMI 1640 cell culture medium supplemented with 10% fetal calf serum, 1% L-glutamine, and 1% penicillin–streptomycin. The medium was changed twice weekly and the cells were passaged at confluency and harvested during the exponential growth phase. Cells between passages 15 and 25 were selected by rinsing the monolayer with 0.02% ethylenediaminetetraacetic acid solution in PBS. After removing the rinsing fluid, the cells were incubated with 0.25% trypsin for approximately 3 min and then resuspended in culture medium and centrifuged at 170g for 3 min. The supernatant was removed, and the cells were resuspended in fresh medium. A Bürker hemacytometer was used for cell counting. The cells were then used either for in vitro binding studies or intraperitoneally injected into the nude mice.

## Immunoreactive Fraction

After radiolabeling, the immunoreactivity of the mAbs was analyzed in vitro by determination of the immunoreactive fraction,  $r$ . A fixed amount of MX35 (10 ng in 0.040 mL medium [1.7 nmol/L]) was added to single-cell suspensions of OVCAR-3 cells, in duplicate, to a final volume of 0.540 mL. The cells were suspended in supplemented cell culture medium at 7 different concentrations, ranging from 5 to 0.078 million per mL. After incubation with gentle agitation for 2 h at room temperature, the cells were centrifuged and rinsed twice in PBS. Specific binding to the cells was determined by radioactivity measurements of the rinsed pellets in a  $\gamma$ -counter (Wizard 1480; Wallace Oy). The value of  $r$ , representing conditions of infinite antigen excess, was finally derived from a plot of total applied radioactivity divided by cell-bound radioactivity as a function of the inverse of the cell concentration, as described by Lindmo et al. (23). The analysis of MOv18 was performed as described above but fixed cells were used due to shedding of the antigen, as described previously (12).

## Kinetic and Equilibrium Constants

To determine the apparent equilibrium association constant,  $K_a$ , and  $B_{\max}$ , Scatchard analysis assays were set up as described by Lindmo et al. (23). Increasing amounts of mAbs were added to a fixed amount of cells in suspension. The radiolabeled mAbs were serially diluted (1:2) in culture medium at 7 concentrations (ranging from 4,000 to 62.5 ng/mL [668–10.4 nmol/L]), 0.040 mL of which was added to the cells in duplicate (100,000 cells in 0.010 mL). Incubation was allowed to proceed for 3 h under the conditions mentioned. Values of  $K_a$  and  $B_{\max}$  were determined from the Scatchard plots, in which corrections had been made for the corresponding value of  $r$ .

The  $k_{\text{on}}$  was determined by adding 10 ng (0.067 pmol) of radiolabeled mAbs, in duplicate, to 2.5 million cells, in a final volume of 0.140 mL (conditions as for the assay of the  $r$ ). The incubation time ranged from 0.5 to 570 min and was interrupted by the removal of unbound radioactivity from the cells, using the centrifugation and rinsing procedure described above. Specific binding to the cells was measured and plotted as the amount of cell-bound radioactivity divided by the amount added as a function of incubation time. The

binding data were then globally fitted to the reaction mechanism equation  $[B] = r \cdot [T] \cdot (1 - \exp(-k_{\text{on}} \cdot [F] \cdot t))$ , where  $[B]$  and  $[T]$  are the concentrations of bound and total amount of mAbs (mol/L), respectively;  $r$  is the immunoreactive fraction;  $k_{\text{on}}$  is the association rate constant ( $1/[\text{mol/L}] \times 1/\text{s}$ );  $[F]$  is the concentration of free antigen (mol/L); and  $t$  is the incubation time (s).

## Dosimetric Calculations

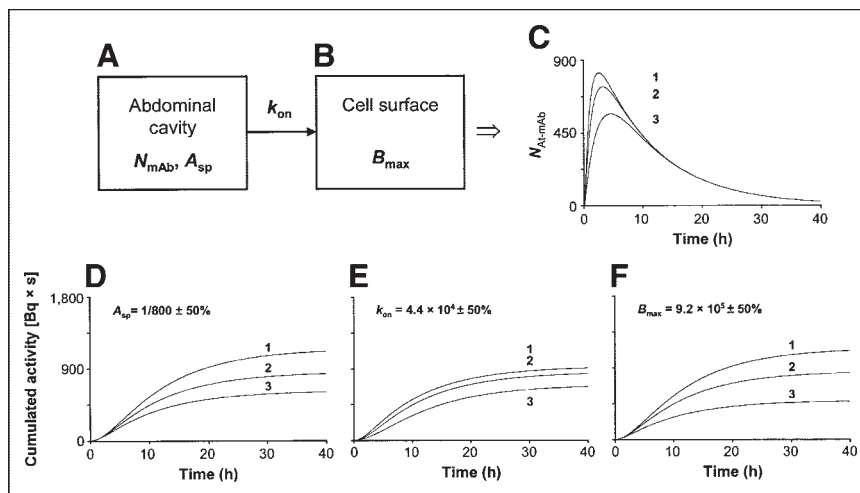
The absorbed dose to tumor cells on the peritoneal surface was calculated for various assumed cluster sizes and radionuclide distributions. The clusters were assumed to be spheric, with a packing ratio of 1. For cell clusters of the selected radii, 25, 50, and 100  $\mu\text{m}$ , the number of cells,  $n_{\text{cell}}$ , will then be 46, 364, and 2,915, respectively ( $r_{\text{cell}} = 7.0 \mu\text{m}$ ). Consequently, the number of antigenic sites in the whole cluster volume was assumed to be  $B_{\max} \times n_{\text{cell}}$ , and the number of sites on the cluster surface was assumed to be  $B_{\max} \times (\text{cluster sphere area}/\text{cell area})$ .

To be able to calculate the absorbed dose, a dynamic compartment model was constructed, which enabled the computation of the cumulated activity on 1 tumor cell. The model was constructed in the commercially available software STELLA (ISEE Systems Inc.). Two compartments were defined: one representing the injected volume and the number of mAbs in the abdominal cavity, and one representing the number of mAbs bound to the antigenic sites of one selected tumor cell (Fig. 1). The initial value in the first compartment was  $N_{\text{mAb}}$ —that is, the total number of intraperitoneally injected mAbs at  $t = 0$ . The transition of mAbs from the first compartment to the second compartment was determined using the in vitro measured  $k_{\text{on}}$ —that is, the rate at which mAbs are bound to the antigenic sites on the cell surface per unit time for a specific antigen concentration. The effect of the gradual saturation of the antigenic sites with time was considered by introducing a gradual reduction in the number of free sites from  $B_{\max}$  to zero into the calculations. According to the conditions during the determination of the kinetic and equilibrium constants, the dissociation rate constant,  $k_{\text{off}}$ , was negligible. During the period of binding and irradiation, a constant concentration of mAbs in the abdominal fluid was assumed. For determination of the cumulated activity of surface-bound mAbs, the number of  $^{211}\text{At}$  atoms on the cell surface at different times was calculated using the  $A_{\text{sp}}$  of the labeled mAbs (134 kBq/ $\mu\text{g}$  [1 labeled mAb out of 800 mAbs] at  $t = 0$ ). The same procedure was adopted for the unbound mAbs in the abdominal fluid, also contributing to the irradiation of the cells.

Previously described software (15) was modified for dosimetry on cell clusters. This software uses stopping-power values of  $\alpha$ -particles in liquid water (16) for Monte Carlo–derived microdosimetry. The 2 main  $\alpha$ -particle energies were taken into consideration—that is, the 5.87-MeV  $\alpha$ -particle (41.7% probability per  $^{211}\text{At}$  decay) released instantaneously on the decay of  $^{211}\text{At}$ , and the 7.45-MeV (58.3%)  $\alpha$ -particle from the decay of the daughter  $^{211}\text{Po}$ . The direction of the  $\alpha$ -particles was selected using a random number generator ( $0 \leq R < 1$ ) for 2 angles in spheric coordinates,  $\Phi = 2\pi R$  and  $\Theta = \arccos(1 - 2R)$ . The software was designed to simulate the energy deposition and  $\alpha$ -particle track length for each 0.01  $\mu\text{m}$  in a defined target volume—here a 5.6- $\mu\text{m}$ -radius sphere—simulating a single tumor cell nucleus embedded at various depths in the tumor cell cluster.

Spheric cell clusters of 25-, 50-, and 100- $\mu\text{m}$  radius were simulated. The first 2 cluster simulations were set in  $(256 \mu\text{m})^3$  cubic matrices, and the last one was set in a  $(350 \mu\text{m})^3$  matrix. The target, the cell nucleus, remained at the center of this matrix to

**FIGURE 1.** Schematic illustration of dynamic compartment model and cumulated activity [Bq × s] curves for 1 tumor cell. (A and B) Compartments A and B represent the number of mAbs in the abdominal cavity and the number of mAbs bound to the cell surface of 1 tumor cell, respectively.  $N_{mAb}$  is the total number of mAbs injected intraperitoneally at  $t = 0$  in 0.7 mL PBS.  $A_{sp}$  is the fraction of mAbs carrying an  $^{211}\text{At}$  atom. The  $k_{on}$  expresses the rate at which mAbs will bind to antigenic sites for a specific antigen concentration. It is assumed in the model that the mAbs are immediately and homogeneously mixed in the abdominal cavity after injection. (C) Illustration of how the reaction rate is affected by the number of mAbs injected by plotting the number of  $^{211}\text{At}$ -mAbs ( $N_{At-mAb}$ ) bound to the cell surface as a function of time in the case of 1,200 (curve 1), 800 (curve 2), and 400 (curve 3) kBq of  $^{211}\text{At}$ -MX35 injected. (D–F) Curve 2 shows the cumulated activity on 1 tumor cell surface as a function of time after injecting 400 kBq of  $^{211}\text{At}$ -MX35. Curves 1 and 3 show the effect on the cumulated activity for a change of +50% and –50%, respectively, in the in vitro determined parameters  $A_{sp}$ ,  $k_{on}$ , and  $B_{max}$ , a situation not unlikely to occur in an in vivo situation.



include the full range of those  $\alpha$ -particles that could contribute to the number of events in the target. To simulate the differing positions in the nucleus of interest, the coordinates for the surrounding cell cluster were then placed correspondingly off-center. For each cell cluster size, at least 5 target positions were selected along the central axis of the sphere. The software was run for at least 1,000 recorded  $\alpha$ -particle events in each target. The mean specific energy at each target position was assigned the corresponding cluster shell. Separate simulations were made to calculate the specific-energy contribution of surrounding unbound  $^{211}\text{At}$ -mAbs circulating freely in the abdominal fluid.

#### Animals and Study Groups

Fifty-three female nude BALB/c *nu/nu* mice (Mollegaard & Bomholtgaard) were used. The animals were housed at 22°C and 50%–60% humidity with a light/dark cycle of 12 h. They were given standard autoclaved pellets and water ad libitum. The animals were allowed to adapt for at least 1 wk after purchase and were then divided into 6 groups and treated as shown in Table 1.

The experiments were approved by the Ethics Committee of Göteborg University.

#### Procedures

At the age of 5 wk, the animals were inoculated intraperitoneally with  $1 \times 10^7$  OVCAR-3 cells suspended in 0.2 mL medium. Three weeks later, still without macroscopic tumors (i.e., tumors visible to the naked eye) on the peritoneum, the animals were injected intraperitoneally with 0.7 mL PBS with or without  $^{211}\text{At}$ -mAbs as indicated in Table 1. The choice of the activity levels in this study was based on a previous study (24) in which the myelotoxicity was investigated during intraperitoneal and intravenous injections of  $^{211}\text{At}$ -mAbs. In that study a myelotoxic limit was reached at about 1,300 kBq of  $^{211}\text{At}$ -mAbs injected intraperitoneally, above which the animals succumbed to severe myelosuppression. Therefore, the highest activity level used in this study was set to 1,200 kBq (range, 1,167–1,211 kBq). Also, the lowest activity level used in this study was set to 400 kBq (MX35: range, 389–422 kBq; MOv18: range, 377–419 kBq) because we wanted

**TABLE 1**  
Study Groups and Number of Mice with Macroscopic and Microscopic Tumors and Ascites

Group	<i>n</i>	Treatment	Activity (kBq)	Macroscopic tumor	Microscopic tumor	Ascites	TFF* (%)
1	9	PBS	—	6/9	9/9	9/9	0
2	9	MX35 in PBS	—	6/9	9/9	9/9	0
3	10	$^{211}\text{At}$ -MOv18 in PBS	377–419	0/10	3/10	0/10	70
4	10	$^{211}\text{At}$ -MX35 in PBS	389–422	0/10	2/10	1/10	80
5	10	$^{211}\text{At}$ -MX35 in PBS	774–808	0/10	4/10	2/10	50
6	5	$^{211}\text{At}$ -MX35 in PBS	1,167–1,211	0/5	2/5	0/5	60

\*TFF = tumor-free fraction (i.e., no macroscopic and microscopic tumors and no ascites).

The presence of macroscopic tumors and ascites was assessed by careful ocular inspection during dissection 2 mo after administration of the different regimes. Microscopic tumor growth was assessed by histopathologic methods using paraffin-embedded biopsies stained with eosin–hematoxylin and microscopy at 40× magnification.

to compare the therapeutic efficacy of our new mAb, MX35, with that used in our previous studies, MOv18 (11–13). Finally, one additional activity level was selected at 800 kBq (range, 774–808 kBq) lying in between these 2 levels. After the injection the general condition of the animals was followed daily. Two months after treatment they were sacrificed and dissected. The presence of ascites and macroscopic tumors was assessed by careful ocular inspection of each animal. Multiple biopsies were taken from the peritoneal surface from all mice and fixed in formalin. These were then dehydrated with xylene, embedded in paraffin, cut into 4- $\mu$ m-thick slices, and stained with eosin–hematoxylin for conventional histopathologic examination. The presence of microscopic tumor growth was rigorously estimated for all biopsies by light microscopy with a magnification of up to 40 $\times$ . The estimation of ascites and macroscopic and microscopic tumors was performed without knowledge of the treatment administered.

## RESULTS

All animals in the 2 control groups (groups 1 and 2) developed ascites and microscopic tumor growth, and 12 of 18 (67%) also had macroscopic peritoneal tumor nodules (Table 1). Thus, there is no evidence of an antineoplastic effect of the nonastatinated mAb. Mice treated with 389–422 kBq (group 4), 774–808 kBq (group 5), or 1,167–1,211 kBq (group 6)  $^{211}\text{At}$ -MX35 did not develop macroscopic tumors, and only 10%, 20%, and 0% of the animals developed ascites in these groups, respectively. Also, microscopic growth was seen in 20%, 40%, and 40% of the animals in these groups, respectively. No relationship between administered activity and response was evident. Treatment with  $^{211}\text{At}$ -MOv18 (377–419 kBq [group 3]) resulted in the same inhibition of growth as the same amount of activity bound to MX35. The general condition of all animals seemed unaffected by the different treatment regimes, although the weights of the treated animals differed significantly from those of the control animals. The mean values  $\pm$  SEM at the time of dissection were 27.1  $\pm$  0.8, 28.0  $\pm$  0.9, 23.4  $\pm$  0.5, 22.1  $\pm$  0.6, 23.8  $\pm$  0.4, and 24.2  $\pm$  0.6 g for groups 1–6, respectively.

The  $r$ , the association rate constant,  $k_{\text{on}}$ , and  $B_{\text{max}}$ , the maximal number of mAbs bound to an OVCAR-3 cell, for the mAb MX35 were determined to be (mean  $\pm$  SEM) 0.82  $\pm$  0.03 (MOv18: 0.80  $\pm$  0.06),  $4.4 \times 10^4 \pm 0.3 \times 10^4$  1/[mol/L]  $\times$  1/s and  $9.2 \times 10^5 \pm 2.1 \times 10^5$ , respectively. During the long-term binding tests (9.5 h), the off-rate was <2%/h. No such data were obtained from mAb MOv18 because of shedding of the antigen in vitro.

The result of the calculations using the dynamic compartment model and the experimentally determined values of  $A_{\text{sp}}$ ,  $k_{\text{on}}$ , and  $B_{\text{max}}$ , are shown in Figure 1. The number of  $^{211}\text{At}$ -mAbs bound to 1 tumor cell increases for 2–4 h until a maximum is reached because of saturation and decay of the radionuclide (Fig. 1C). Also, the increase of the reaction rate (i.e., the number of cell-bound  $^{211}\text{At}$ -mAbs [ $N_{\text{At-mAb}}$ ] per time interval) as the injected activity is increased is also illustrated, resulting in an increased maximal value of  $N_{\text{At-mAb}}$ : 560, 730, and 820 for 400 (Fig. 1C, curve 3), 800 (Fig.

1C, curve 2), and 1,200 kBq injected (Fig. 1C, curve 1), respectively.

Figures 1D–1F (curve 2) show the cumulated activity calculated for 400-kBq of  $^{211}\text{At}$ -mAb and the experimentally obtained values for  $A_{\text{sp}}$ ,  $k_{\text{on}}$ , and  $B_{\text{max}}$ . Almost all  $^{211}\text{At}$  atoms decay within 24 h, resulting in a cumulated activity of about 800 Bq  $\times$  s on the cell surface after 24 h. Figure 1 also illustrates calculations of the cumulated activity for other values of  $A_{\text{sp}}$ ,  $k_{\text{on}}$ , and  $B_{\text{max}}$ . For example, an increase in  $A_{\text{sp}}$  of 50% increases the cumulated activity by  $\sim$ 30% (Fig. 1D, curve 1), whereas an increase in  $k_{\text{on}}$  of 50% has very little influence (Fig. 1E, curve 1).

The absorbed dose originating from mAbs bound to the antigenic sites on the tumor cells (the specific contribution) and that originating from mAbs not bound to the tumor cells but freely circulating in the abdominal cavity (the nonspecific contribution) are presented in Figure 2. In the case in which the  $^{211}\text{At}$ -mAbs are assumed to be homogeneously distributed throughout the whole cell cluster, the absorbed dose is very high and varies between 126 and 731 Gy for 400 kBq of  $^{211}\text{At}$ -MX35 ( $r_{\text{cluster}} = 25 \mu\text{m}$ ) and 1,200 kBq of  $^{211}\text{At}$ -MX35 ( $r_{\text{cluster}} = 100 \mu\text{m}$ ), respectively. The absorbed dose in situations in which the  $^{211}\text{At}$ -mAbs are only situated on the surface of the cell cluster or freely circulating around the cluster is considerably lower but, in most cases, still high. For example, for the cluster-surface distributed  $^{211}\text{At}$ -MX35, the absorbed dose never falls below 29 Gy for the cell cluster with 25- $\mu\text{m}$  radius. The minimum value for the nonspecific absorbed dose contribution for this cell cluster never falls below 16 Gy, as can be estimated from Figure 2.

## DISCUSSION

Primary tumors frequently disseminate long before being diagnosed and, thus, local therapy will fail. Therefore, adjuvant systemic therapy for occult micrometastatic disease has become routine in clinical oncology. Standard chemotherapy currently used is not specific to tumor cells and is frequently ineffective because of cellular resistance mechanisms. Targeted therapy not hampered by resistance to cytotoxic drugs has long been the goal of oncologists, and the advent of mAbs seems to provide a suitable tool. Cytotoxicity can be mediated either by direct immunotoxicity or by binding radionuclides to mAbs.

In the present study we used a tumor model relevant in clinical oncology—ovarian cancer, most frequently lethal in spite of complete clinical remission after surgery and chemotherapy. The model is of particular interest because the disease is usually restricted to the peritoneal surfaces and the patient succumbs because of advanced peritoneal tumor growth, including ascites. A model in mice mimicking the human disease is available and has often been used for the development of new therapeutic strategies (11–13). Thus, the clinical disease and the model allow regional treatment, sparing the subject from myelotoxicity.

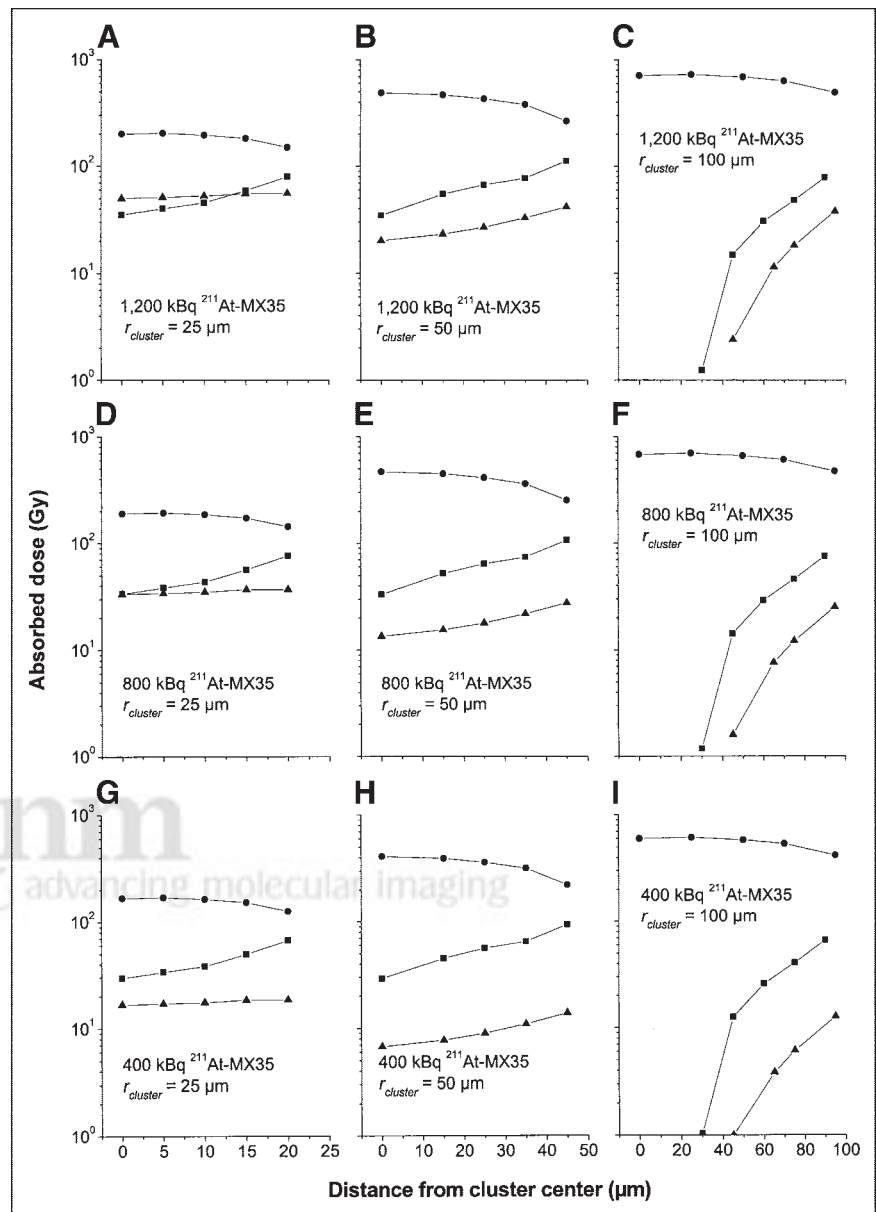


**FIGURE 2.** The absorbed dose at different distances from the center of the differently sized tumor cell clusters ( $r_{cluster} = 25$  [A, D, and G], 50 [B, E, and H], and 100 [C, F, and I]  $\mu m$ ) illustrated for the 3 different activity levels used (1,200 [A–C], 800 [D–F], and 400 [G–I] kBq) for 3 cases: <sup>211</sup>At-MX35 homogeneously distributed over all cell surfaces throughout the whole cell cluster (●), <sup>211</sup>At-MX35 homogeneously distributed only on the cell surfaces defining the surface of the cell cluster (■), and <sup>211</sup>At-MX35 homogeneously distributed in the abdominal fluid (no specific binding to the tumor cells at all) (▲).

Several studies with <sup>90</sup>Y-, <sup>131</sup>I-, <sup>177</sup>Lu-, or <sup>186</sup>Re-labeled mAbs have been performed both in animals and in humans with rather poor results (1–8). McQuarrie et al. (1) recently performed studies in nude mice xenografted with OVCAR-3 cells using intraperitoneal regimens with the combination of a bispecific anti-CA 125 mAb and <sup>90</sup>Y-labeled biotinylated long-circulating liposomes as a potential adjuvant treatment. A median tumor growth delay of 91 d compared with 77 d for the control group was observed. Janssen et al. (2) studied the therapeutic efficacy of RIT using the murine mAb HMFG1 labeled with <sup>90</sup>Y, <sup>131</sup>I, or <sup>186</sup>Re in nude mice with intraperitoneally growing OVCAR-3 ovarian carcinoma xenografts. Each of the 3 regimens caused a delay in ascites formation and mortality as compared with the control groups treated with <sup>90</sup>Y-labeled irrelevant mAb, nonradiolabeled HMFG1, or PBS.

They also concluded that intraperitoneally administered <sup>90</sup>Y-HMFG1 more effectively inhibited tumor growth than intravenously administered <sup>90</sup>Y-HMFG1. Borchardt et al. (3) studied the therapeutic efficacy in nude mice bearing intraperitoneal nodules of SK-OV-3 NMP2 by intraperitoneal administration of an <sup>90</sup>Y-labeled human IgM. The mice received a single administration or fractionated administrations of <sup>90</sup>Y-2B12. Untreated mice and mice treated with unlabeled immunoconjugates served as controls. The controls had a mean survival time of 20 and 17 d, respectively. Treatment with <sup>90</sup>Y-2B12 increased median survival by 11–12 d per 3.7 MBq (100  $\mu Ci$ ) for a single administration (~1.8–14.8 MBq [50–400  $\mu Ci$ ]) and fractionated administrations (~5.6–18.9 MBq [150–510  $\mu Ci$ ]). Rather good therapeutic results were achieved by Horak et al. (25) using the  $\alpha$ -emitter <sup>212</sup>Pb on intraperitoneally injected SK-OV-3

cells. Three days after cell inoculation,  $^{212}\text{Pb}$ -labeled anti-HER2/neu mAb AE1 was administered intravenously. A prolonged tumor-free survival was noted in the mice compared with those given no treatment or those treated with the unlabeled mAb.

However, conventional  $\beta$ -emitting radionuclides used in the cited studies have a range that is too long to effectively irradiate microscopic tumors but also have a half-life that is too long to be optimal for intraperitoneal use.  $^{211}\text{At}$ , with its short particle range and relatively short half-life, seems to be an ideal radionuclide when the tumors are microscopic and restricted to the peritoneal surfaces. Therefore, we believe it is of utmost importance to thoroughly investigate the therapeutic efficacy using this  $\alpha$ -particle emitter labeled to mAbs when treating microscopic disease on the peritoneum. To understand and predict the degree of efficacy in our therapy study, the experiments were complemented with dosimetric estimations.

Because it is very difficult to quantify the uptake of  $^{211}\text{At}$ -MX35 in the microscopic tumors *in vivo*, the dosimetry was based on assumed tumor cluster sizes and on studies of the binding kinetics of the radioimmunocomplexes *in vitro*. The study of binding kinetics could not be done for mAb MOv18 because its antigen sheds *in vitro*. From the determined values of the parameters  $k_{\text{on}}$  and  $B_{\text{max}}$ , theoretic uptake curves could be constructed and used for the dosimetry. A constant concentration of the mAbs in the abdominal fluid was assumed during the binding period *in vivo*. This may not be the case *in vivo* because the higher diffusion and convection of water molecules ( $\sim 18$  Da) through the peritoneum rather than the lymphatic drainage of macromolecules ( $\sim 150$  kDa) can lead to an increase in mAb concentration and, thus, increased specific and non-specific absorbed dose contributions. Thus, the calculations based on constant activity concentration give a lower limit of the absorbed dose. However, it should also be noted that a reduction in the mAb concentration with time might be possible. If the number of tumor cells capable of binding the mAbs is very large and if the number of mAbs that can bind to a cell *in vivo* is in the order of  $B_{\text{max}}$  measured *in vitro*, the mAbs will be consumed and the concentration decreased. Preliminary calculations indicate that a successive increase or decrease of the mAb concentration in the abdominal cavity has little effect on the cumulated activity on a tumor cell, justifying our assumption of a constant mAb concentration.

Calculations of the absorbed dose originating from specific binding of the mAbs to the antigenic sites of the tumor cells were performed for optimal conditions—that is, assuming that all tumor cells and antigenic sites in a tumor cell cluster are available to the mAb and that immediate mixing in the abdominal cavity and free diffusion of the mAbs into the tumor tissue occur. This situation may not occur *in vivo* but was assumed for the purpose of estimating the maximal attainable absorbed dose to the tumor cells. Further studies must investigate the diffusion and distribu-

tion of mAbs in microscopic tumor clusters. The absorbed dose contribution to a cell cluster was also calculated for the other extreme—no diffusion into the tumor—resulting in an  $^{211}\text{At}$ -mAb distribution only on the surface of the cluster. This means that the radiation will not reach the inner part when the cluster is greater than  $\sim 71$   $\mu\text{m}$  in radius, corresponding to the maximal pathlength of the  $\alpha$ -particles in tissue. However, for smaller tumors, the mean absorbed dose is surprisingly high, indicating that there is no absolute need for the mAbs to penetrate the tumor. An absorbed dose of  $>15$  Gy can be regarded as high, considering the high biologic effect of the  $\alpha$ -particles. In a previous study (10), *in vitro* irradiation of OVCAR-3 cells using  $^{211}\text{At}$  gave a  $D_{37}$  (mean absorbed dose required for 37% cell survival) of 0.56 Gy, indicating a very high probability of tumor eradication at 15 Gy. Internalization of the mAb into the tumor cell alters the dosimetric estimates, especially for the single cell situation. However, the results of the long-term *in vitro* binding test show a stable cell uptake of  $^{211}\text{At}$  during 9.5 h, indicating insignificant internalization (26).

The dissection of the animals 2 mo after the injection of approximately 400–1,200 kBq of  $^{211}\text{At}$ -MX35 showed a tumor-free fraction (TFF)—that is, no macroscopic and microscopic tumors and no ascites—of 50%–80%. It is not possible to administer higher activity because of the irradiation of the bone marrow, resulting in severe hematologic toxicity (24). However, the TFF was not correlated with the administered activity. This can be explained by the saturation of antigenic sites, which—according to our dynamic compartment model—occurs within a few hours after the injection, resulting in a similar absorbed dose for the 3 activity levels. The results using  $^{211}\text{At}$ -MOv18 showed a similar TFF, 70%. This value is also in agreement with the results of a previous study using  $^{211}\text{At}$ -MOv18 and the same tumor model (11). In that study, a nonspecific  $^{211}\text{At}$ -mAb was also used (C242), showing some therapeutic effect. According to the dose calculations in the present study, the absorbed dose from a nonspecific (unbound) mAb is at least 7 Gy for 400 kBq of  $^{211}\text{At}$ -mAb, for cell clusters  $<71$   $\mu\text{m}$  in radius. Considering the high radiosensitivity of the tumor cells to the  $\alpha$ -particle irradiation, the effect of a nonspecific mAb is expected to be considerable.

The dynamic compartment model was used to illustrate how the cumulated activity is affected by the  $k_{\text{on}}$  and  $B_{\text{max}}$ . The results showed that  $B_{\text{max}}$  was most critical. An increase in  $B_{\text{max}}$  of 50%, from  $9.2 \times 10^5$  to  $1.38 \times 10^6$  mAbs bound per cell, would result in an increase in the cumulated activity of  $\sim 25\%$ . This can be compared with an increase in  $k_{\text{on}}$  of 50%, from  $4.4 \times 10^4$  to  $6.6 \times 10^4$   $1/[\text{mol/L}] \times 1/\text{s}$ , yielding an increase in the cumulated activity of only  $\sim 10\%$  (Fig. 1). Also, if  $A_{\text{sp}}$  could be increased 50%, from 1  $^{211}\text{At}$ -mAb in every 800 mAbs (1:800) to 1:533, this would increase the cumulated activity by  $\sim 30\%$  (Fig. 1), indicating a possibility to improve the therapeutic outcome.

Considering the absorbed doses presented in Figure 2, they are generally high, especially when an RBE of 3–5 is

considered. However, as it was seen in the case of the cell cluster with a radius of 100  $\mu\text{m}$ , the absorbed dose falls to zero at a distance of  $\sim 30$   $\mu\text{m}$  from the center of the cluster, when the  $^{211}\text{At}$ -mAb is assumed to be located only at the surface of the tumor cell cluster or circulating in the fluid surrounding it (nonspecific contribution). This could partially explain the number of unsuccessfully treated mice, indicating the presence of large cell clusters—that is, clusters with radii exceeding the maximum range of the  $\alpha$ -particles ( $\sim 71$   $\mu\text{m}$ ), at the time of treatment—together with poor penetration of the mAbs. This will be investigated further in a forthcoming study in which treatment will be given at different times after tumor cell inoculation accompanied by a microscopic analysis of tumor size. For large cell clusters that have developed blood vessels, there may also be a radiation effect from  $^{211}\text{At}$ -mAbs that have passed into the circulation. This contribution to the tumor dose was not considered in our dose calculation, as it is difficult to estimate the mAb uptake in these small tumors. However, preliminary studies indicate no vascularization of microscopic tumor clusters (radii,  $< 60$   $\mu\text{m}$ ) of OVCAR-3 cells in nude mice. If  $^{211}\text{At}$  is to be used for macroscopic tumors, a pretargeting approach seems to be necessary, as fast tumor uptake is mandatory for a short-lived radionuclide.

Another concern regarding intraperitoneal RIT is the distribution of the injected activity in the abdominal cavity. It is uncertain whether the injected solution will gain access to the entire abdominal cavity. Adhesion between peritoneal surfaces including tumor cells, as well as resulting compartmentalization, may result in areas and volumes inaccessible to the mAbs. This is not unlikely in the clinical situation in which prior surgery could compartmentalize the abdominal cavity, making the therapeutic outcome more uncertain. Another problem in the animal model, although rather unlikely, is unintentional intraintestinal injections. However, if this should happen, the absorbed dose would be reduced because of rapid drainage of the injected activity through the intestines.

## CONCLUSION

The use of the high-LET, short-range  $\alpha$ -particle emitter  $^{211}\text{At}$  labeled to the mAb MX35 and intraperitoneally injected exhibits a high efficacy when treating micrometastatic growth of the ovarian cancer cell line OVCAR-3 on the peritoneum of nude mice. The TFF was in the mean 64% after the injection of  $\sim 400$ – $1,200$  kBq of  $^{211}\text{At}$ -MX35. The result is comparable with the present as well the previous studies using  $^{211}\text{At}$ -MOv18. The calculated absorbed doses, based on the biokinetic model and Monte Carlo simulation, are high for tumor sizes less than  $\sim 71$   $\mu\text{m}$  in radius, explaining the favorable therapeutic outcome. The lack of an activity–response relationship between 400 and 1,200 kBq is explained by antigenic site saturation of unlabeled mAbs. Consequently, increased specific activity could be a way to further improve the therapeutic outcome.

The results obtained in this study, together with those obtained earlier, indicate that a phase I clinical study is justified and, consequently, will soon be initiated.

## ACKNOWLEDGMENTS

This work was supported by grants from the Swedish Cancer Foundation (project 3548) and the King Gustaf V Jubilee Clinic Research Foundation in Göteborg, Sweden.

## REFERENCES

- McQuarrie S, Mercer J, Syme A, Suresh M, Miller G. Preliminary results of nanopharmaceuticals used in the radioimmunotherapy of ovarian cancer. *J Pharm Pharmacol Sci.* 2005;7:29–34.
- Janssen ML, Pels W, Massuger LF, et al. Intraperitoneal radioimmunotherapy in an ovarian carcinoma mouse model: effect of the radionuclide. *Int J Gynecol Cancer.* 2003;13:607–613.
- Borchardt PE, Quadri SM, Freedman RS, Vriesendorp HM. Intraperitoneal radioimmunotherapy with human monoclonal IgM in nude mice with peritoneal carcinomatosis. *Cancer Biother Radiopharm.* 2000;15:53–64.
- Grana C, Bartolomei M, Handkiewicz D, et al. Radioimmunotherapy in advanced ovarian cancer: Is there a role for pre-targeting with  $^{90}\text{Y}$ -biotin? *Gynecol Oncol.* 2004;93:691–698.
- Meredith RF, Alvarez RD, Partridge EE, et al. Intraperitoneal radioimmunotherapy of ovarian cancer: a phase I study. *Cancer Biother Radiopharm.* 2001;16:305–315.
- Mahe MA, Fumoleau P, Fabbro M, et al. A phase II study of intraperitoneal radioimmunotherapy with iodine-131-labeled monoclonal antibody OC-125 in patients with residual ovarian carcinoma. *Clin Cancer Res.* 1999;5(suppl):3249–3253.
- Epenetos AA, Hird V, Lambert H, Mason P, Coulter C. Long term survival of patients with advanced ovarian cancer treated with intraperitoneal radioimmunotherapy. *Int J Gynecol Cancer.* 2000;10:44–46.
- Stewart JSW, Hird V, Snook D, et al. Intraperitoneal yttrium-90-labeled monoclonal antibody in ovarian cancer. *J Clin Oncol.* 1990;8:1941–1950.
- Andersson H, Elgqvist J, Horvath G, et al. Astatine-211-labeled antibodies for treatment of disseminated ovarian cancer: an overview of results in an ovarian tumor model. *Clin Cancer Res.* 2003;9:3914–3921.
- Palm S, Andersson H, Bäck T, et al. In vitro effects of free  $^{211}\text{At}$ ,  $^{211}\text{At}$ -albumin and  $^{211}\text{At}$ -monoclonal antibody compared to external photon irradiation on two human cancer cell lines. *Anticancer Res.* 2000;20:1005–1012.
- Andersson H, Lindegren S, Bäck T, Jacobsson L, Leser G, Horvath G. Radioimmunotherapy of nude mice with intraperitoneally growing ovarian cancer xenograft utilizing  $^{211}\text{At}$ -labelled monoclonal antibody MOv18. *Anticancer Res.* 2000;20:459–462.
- Andersson H, Lindegren S, Bäck T, Jacobsson L, Leser G, Horvath G. The curative and palliative potential of the monoclonal antibody MOv18 labelled with  $^{211}\text{At}$  in nude mice with intraperitoneally growing ovarian cancer xenografts: a long term study. *Acta Oncol.* 2000;39:741–745.
- Andersson H, Palm S, Lindegren S, et al. Comparison of the therapeutic efficacy of  $^{211}\text{At}$ - and  $^{131}\text{I}$ -labelled monoclonal antibody MOv18 in nude mice with intraperitoneal growth of human ovarian carcinoma. *Anticancer Res.* 2001;21:409–412.
- Rubin SC, Kostakoglu L, Divgi C, et al. Biodistribution and intraoperative evaluation of radiolabeled monoclonal antibody MX35 in patients with epithelial ovarian cancer. *Gynecol Oncol.* 1993;51:61–66.
- Palm S, Humm JL, Rundqvist R, Jacobsson L. Microdosimetry of astatine-211 single-cell irradiation: role of daughter polonium-211 diffusion. *Med Phys.* 2004;31:218–225.
- ICRU. *Stopping Powers and Ranges for Protons and Alpha Particles.* Publication 49. Bethesda, MD: International Commission on Radiation Units and Measurements; 1993.
- Lindegren S, Bäck T, Jensen H. Dry-distillation of astatine-211 from irradiated bismuth targets: a time-saving procedure with high recovery yields. *Appl Radiat Isot.* 2001;55:157–160.
- Welshinger M, Yin BWT, Lloyd KO. Initial immunochemical characterization of MX35 ovarian cancer antigen. *Gynecol Oncol.* 1997;67:188–192.

19. Miotti S, Canevari S, Me'nard S, et al. Characterisation of human ovarian carcinoma associated antigens defined by novel monoclonal antibodies with tumor-restricted specificity. *Int J Cancer*. 1987;39:297–303.
20. Boerman OC, van Niekerk CC, Makkink K, et al. Comparative immunohistochemical study of four monoclonal antibodies directed against ovarian carcinoma associated antigens. *Int J Gynecol Pathol*. 1991;10:15–25.
21. Lindgren S, Andersson H, Bäck T, Jacobsson L, Karlsson B, Skarnemark G. High-efficiency astatination of antibodies using N-iodosuccinimide as the oxidizing agent in labeling of N-succinimidyl 3-(trimethylstannyl)benzoate. *Nucl Med Biol*. 2001;28:33–39.
22. Hamilton TC, Young RC, McKoy WM, et al. Characterization of a human ovarian carcinoma cell line (NIH:OVCAR-3) with androgen and estrogen receptors. *Cancer Res*. 1983;43:5379–5389.
23. Lindmo T, Boven E, Cuttitta F, et al. Determination of the immunoreactive fraction of radiolabeled monoclonal antibodies by linear extrapolation to binding at infinite antigen excess. *J Immunol Methods*. 1984;72:77–89.
24. Elgqvist J, Bernhardt P, Hultborn R, et al. Myelotoxicity and RBE of  $^{211}\text{At}$ -conjugated mAbs compared with  $^{99\text{m}}\text{Tc}$ -conjugated mAbs and  $^{60}\text{Co}$  irradiation in nude mice. *J Nucl Med*. 2005;46:464–471.
25. Horak E, Hartmann F, Garmestani K, et al. Radioimmunotherapy targeting of HER2/neu oncoprotein on ovarian tumor using lead-212-DOTA-AE1. *J Nucl Med*. 1997;38:1944–1950.
26. Reist CJ, Foulon CF, Alston K, Bigner DD, Zalutsky MR. Astatine-211 labeling of internalizing anti-EGFRvIII monoclonal antibody using N-succinimidyl 5- $^{211}\text{At}$ astato-3-pyridinecarboxylate. *Nucl Med Biol*. 1999;26:405–411.

